Proceedings of the ASME 2014 International Design Engineering Technical Conferences &
Computers and Information in Engineering Conference
IDETC/CIE 2014
August 17-20, 2014, Buffalo, New York, USA

DETC2014-34932

THE ROLE OF THE ORTHOGONAL HELICOID IN THE GENERATION OF THE TOOTH FLANKS OF INVOLUTE-GEAR PAIRS WITH SKEW AXES

Giorgio Figliolini *
Department of Civil & Mechanical Engineering
University of Cassino
Via G. Di Biasio 43, 03043 Cassino (Fr), Italy
E-mail: figliolini@unicas.it

Hellmuth Stachel
Institute of Discrete Mathematics and Geometry
Vienna University of Technology
Wiedner Hauptstr. 8-10/104 – A 1040 Wien, Austria
E-mail: stachel@dmg.tuwien.ac.at

Jorge Angeles
Department of Mechanical Engineering & CIM
McGill University
817 Sherbrooke St. West – Montréal, Québec, H3A 2K6, Canada
E-mail: angeles@cim.mcgill.ca

ABSTRACT

Camus' concept of Auxiliary Surface (AS) is extended to the case of involute gears with skew axes. In the case at hand, we show that the AS is an orthogonal helicoid whose axis a) lies in the cylindroid and b) is normal to the instant screw axis of one gear with respect to its meshing counterpart; in general, the helicoid axis is skew with respect to the latter. According to the spatial version of Camus' Theorem, any line attached to the AS, in particular any generator g of AS itself, can be chosen to generate a pair of conjugate flanks with line contact.

While the pair of conjugate flanks is geometrically feasible, as they always share a line of contact and the tangent plane at each point of this line, there are poses where the flanks even have a common Disteli axis. Then there is a G^2-contact at the striction point and the two surfaces penetrate each other.

The outcome is that the surfaces are not realizable as tooth flanks. Nevertheless, this is a fundamental step towards the synthesis of the flanks of involute gears with skew axes.

Keywords: skew-axis involute gears; Plücker conoid (a.k.a the cylindroid); spatial Camus' Theorem; Ball-Disteli diagram; osculating ruled surfaces.

1 INTRODUCTION

Gears of many types, cylindrical and bevel, with straight and helical teeth, along with hypoid and worm gears, are key components to transmit mechanical power in machines.

They can be assembled to produce simple and planetary gear trains, which also include non-circular gears. The most commonly used tooth profiles are cycloidal and involute, the latter for assembling, manufacturing and dynamic-performance properties.

Camus's theorem provides a universal approach to the synthesis of conjugate profiles when the relative motion program is assigned through the relative centrodes, or via the pitch circles, in the case of a constant transmission ratio. The main point of this approach is to choose the most convenient auxiliary curve, in order to trace the pair of conjugate tooth profiles as trajectories of a point, or to generate them using envelope of a second curve attached to this auxiliary curve.

The first method is normally used to synthesize cycloidal gears, which has been also extended to the spatial case through the use of helicoids as auxiliary surfaces, while the second method is more suitable to generate involute gears. Nevertheless, the extension of Camus' theorem to involute-gear pairs with skew axes is an extremely complex task, although quite interesting, since it is based on the fundamentals of kinematics and thus, targeted to provide a unified theory to synthesize any type of gears.

This paper aims to give a first important contribution in this direction by specifying and analyzing the role of the orthogonal helicoid in the generation of the tooth flanks of involute-gear pairs with skew axes. Cylindrical and bevel gears can be obtained as particular cases. In the planar case, the tooth flanks are not realizable because they are mutually intersecting; nevertheless, this proves that the orthogonal helicoid is the right extension into the space.

* Associate Professor and author of correspondence, Phone: (+39) 0776-2993662, Fax: (+39) 0776-2993704, E-mail: figliolini@unicas.it

2 A BIOSKETCH OF MARTIN DISTELI

Martin Disteli was very active in geometry and kinematics. In particular, he introduced the concept of axis of curvature, which is also known as Disteli axis in his honor; consequently, he extended the Euler-Savary equation to the spatial case and, thus, he applied these concepts to the synthesis of spatial cycloidal gears.

Nevertheless, he is not well known among the research community, specially, among the engineering community, even if he made many important contributions in this field. Referring to [1-10], a biosketch of Martin Disteli is reported below, with the aim to make his life and his career known and to spread his scientific work.

Martin Disteli, whose picture is shown in Fig.1, was born on Sunday, August 5th, 1867 in Olten, Switzerland, the son of a railway-station inspector. Disteli attended elementary school in his hometown; then, he went on to the Cantonal School in Solothurn at the age of 17. The instruction that the young Disteli received in the latter motivated him to devote himself to mathematics. After completing highschool, Disteli registered, the same year, at the Zurich Polytechnic, where he studied mathematics in the Education Department. It didn't take too long for the freshman Disteli to discover his interest in geometry, and found in Wilhelm Fiedler, Professor at the Zurich Institute of Technology, the mentor from whom he would receive key enlightening in mathematics. After four years of study, Disteli completed the first part of his higher education. Right afterwards, he studied two more semesters at the University of Berlin, where Weierstrass was still teaching, followed by further study at the University of Geneva.

In 1887 Disteli went back to Zurich, where he took up a job as assistant of his mentor Wilhelm Fiedler. Since Disteli profited of his two years of travel to work on his doctoral thesis, already by 1888 he was granted the degree of Doctor of Mathematics at the Federal Institute of Technology, in Zurich.

Disteli kept his assistantship still four more years, until he traded it, in 1893, for a professorship of descriptive geometry at the Cantonal Vocational School in Winterthur, where he moved in the same year. Besides this position, Disteli kept a lecturer position in Zurich, and was, additionally, coauthor in numerous scientific publications. The teaching in Winterthur was not a long-term commitment for Disteli, one must say, so that in Easter 1898 he gave up his professorship and his lecturer position in Zurich, to devote himself to his own scientific education. So, Disteli moved to Germany, to the mathematics metropolis of Göttingen, where, among others, David Hilbert and Felix Klein were teaching at the time. His experience in Göttingen was not that positive: not only was pure geometry there abandoned, but also was Disteli now married, which made him feel no longer unconstrained and free to move as he had done earlier. It thus happened that, after one semester, he moved again, towards the south, this time to Strassburg, which then was a part of the German Reich. This time he was accompanied by his wife. From Strassburg it was just one short step until he became in 1899 Assistant and in 1901 Professor (one level below Full Professor, or Ordinarius) at the Karlsruhe Technische Hochschule (Karlsruhe Institute of Technology). In 1902 he moved again to Strassburg to take on a position as Professor of Applied Mathematics.

In 1905 Disteli was granted a Full Professorship of Descriptive Geometry at the Dresden Technische Hochschule. Disteli claimed that this time was the most beautiful of his life. However, this period was not completely peaceful. Far from their hometwon, the Distelis missed their relatives and acquaintances in Switzerland. Martin Disteli must have found it especially painful that his wife and growing son had to spend the school holidays, which happened within the semester, alone in Switzerland. This prompted Disteli to move for the second time to Karlsruhe, where he occupied this time a Full Professorship in Descriptive Geometry. The time in Karlsruhe, however, was obscured by the shadow of the First World War. Disteli's duties at the Karlsruhe Institute of Technology changed dramatically, as his assistants were drafted. Matters became even tougher, as he became so seriously ill that an operation was necessary, given that by virtue of the war cost he could not be cured with a treatment.

Thus decided Disteli to give up his Chair in Karlsruhe and move with his family to war-free Switzerland. This move turned out to be in 1917 harder than anticipated. It is to be noted that because of a call to join the Swiss Army he had to leave Germany and return to his motherland. However, Disteli did not have to enter the Army. Instead, and thanks to the new living conditions, the good care of his family led to a quick recovery. In the winter semester of 1920-21, Disteli succeeded in securing a position at the University of Zurich, where he, among other activities, was responsible for the education of mathematics teachers. In the fall of 1923 his old disease returned. In spite of an immediate operation he could not recover, so that in the night of October 25th to 26th of the same year, Disteli died as a consequence of his illness.

His scientific work inspired important research lines on the theory of curvature and the application of dual algebra in spatial kinematics, [11-14]. One of these topics is the synthesis of skew gears, [15-18].

Figure 1. Martin Disteli

3 PITCH HYPERBOLOIDS AND PLÜCKER CONOID

Referring to Fig.2, a pair of skew gears is assigned through their axes of rotation, I_2 and I_3, for the driving and driven gears, 2 and 3, respectively. I_2 coincides with the Z-axis of the fixed frame $\mathcal{F}_0$ (X, Y, Z), while I_3 is given the distance a_1 along the positive X-axis and the oriented angle α_1.

The instant screw axis I_{32}, ISA for brevity, can be determined through the general Aronhold-Kennedy theorem, which states that I_2, I_3 and I_{32} must share a common normal, the X-axis in this case, as reported in [19]. Thus, the position of the I_{32}-axis is given by the distance b_2 along the X-axis and the oriented angle ϑ_2.

Referring to the formulation proposed in [20-23] and briefly recalled here, the relative angular and point velocities, ω_{32} and v_{32}, respectively, can be expressed in the forms

$$\omega_{32} = \pm\sqrt{1-2k\cos\alpha_1+k^2} \tag{1}$$

and

$$v_{32} = \frac{k\,\omega_3 \sin\alpha_1}{\pm\sqrt{1-2k\cos\alpha_1+k^2}}\,a_1 \tag{2}$$

where $k = \omega_2 / \omega_3$ is the transmission ratio between the pair of skew gears, which is negative for external and positive for internal gears.

Likewise, the position of the ISA in the fixed frame $\mathcal{F}_0$ (X, Y, Z) is given through the oriented angle ϑ_2 and the distance b_2, namely,

$$\tan\vartheta_2 = \frac{\sin\alpha_1}{\cos\alpha_1 - k} \tag{3}$$

$$b_2 = \frac{1-k\cos\alpha_1}{1-2k\cos\alpha_1+k^2}\,a_1 \tag{4}$$

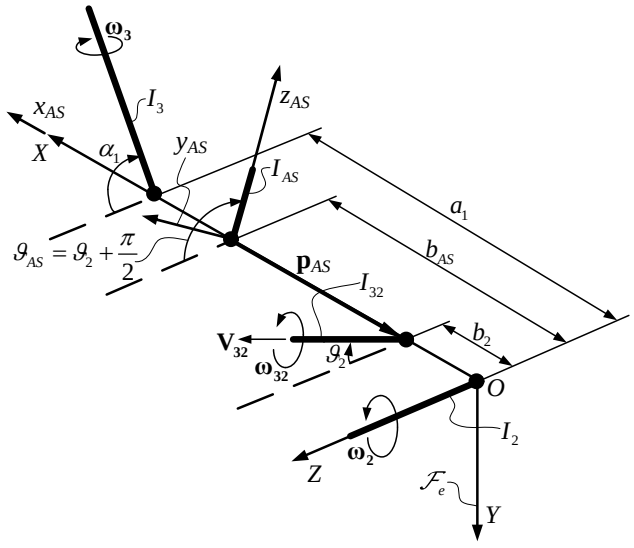

Figure 2. Positions of the I_2 and I_3 axes of both skew gears, along with the I_{32}-axis (ISA) and the I_{AS}-axis of the orthogonal helicoid with respect to the fixed frame $\mathcal{F}_0$ (X,Y,Z)

The hyperboloid pitch surface $\mathcal{P}_2$ of the driving gear 2 can be expressed via two-parameter, ψ and λ, position vector $\mathbf{r}_2$, namely,in the form

$$\mathbf{r}_2(\psi,\lambda) = b_2\begin{bmatrix}\cos\psi\\-\sin\psi\\0\end{bmatrix} + \lambda\begin{bmatrix}-\sin\psi\sin\vartheta_2\\-\cos\psi\sin\vartheta_2\\\cos\vartheta_2\end{bmatrix} \tag{5}$$

where $\lambda \in \mathbb{R}$ and $\mathbf{r}_2$ refers to a point of the line generating the pitch surface.

Likewise, the hyperboloid pitch surface $\mathcal{P}_3$ is given by

$$\mathbf{r}_3(\varphi,\lambda) = d\begin{bmatrix}\cos\varphi\\\sin\varphi\cos\alpha_1\\-\sin\varphi\sin\alpha_1\end{bmatrix} - \lambda\begin{bmatrix}\sin\varphi\sin\beta_1\\\cos\varphi\sin\beta_1\cos\alpha_1-\cos\beta_1\sin\alpha_1\\\cos\varphi\sin\beta_1\sin\alpha_1+\cos\beta_1\cos\alpha_1\end{bmatrix} + \begin{bmatrix}a_1\\0\\0\end{bmatrix} \tag{6}$$

where $d = (b_2 - a_1)$ and $\beta_1 = (\vartheta_2 - \alpha_1)$, which takes into account the translation a_1 along the X-axis and the rotation α_1 with respect to the Z-axis.

Still referring to the formulation proposed in [29-31], the Plücker conoid $\mathcal{C}$ can be expressed in $\mathcal{F}_0$ (X, Y, Z) as

$$\mathbf{r}(\vartheta_2, b_2, \lambda) = \begin{bmatrix}b_2\\0\\0\end{bmatrix} + \lambda\begin{bmatrix}0\\-\sin\vartheta_2\\\cos\vartheta_2\end{bmatrix} \tag{7}$$

where the range of λ can be chosen arbitraly, because it defines only the extension of the Plücker conoid, while the parameters ϑ_2 and b_2 are obtained from Eqs. (3) and (4), respectively, when the transmission ratio k varies in the range $(+\infty; -\infty)$. An example is shown in Fig. 3.

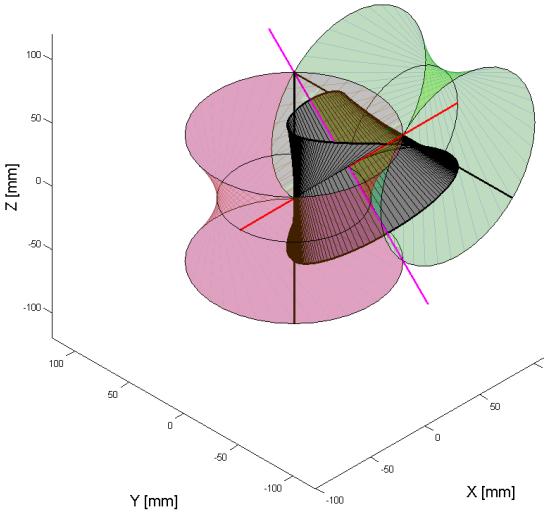

Figure 3. Hyperboloid pitch surfaces $\mathcal{P}_2$ and $\mathcal{P}_3$ along with their Plücker conoid $\mathcal{C}$ for a_1 = 100 mm, α_1 = 90°, k = – 1.

4 SYNTHESIS OF THE ORTHOGONAL HELICOID

According to Camus' theorem for skew gears, a pair of conjugate ruled surfaces with line contact can be obtained by referring to both hyperboloid pitch surfaces $\mathcal{P}_2$ and $\mathcal{P}_3$ of the driving and driven gears, respectively, by choosing a suitable auxiliary surface (AS), which must be tangent to both hyperboloids along the I_{32}-axis, *i.e.* the ISA of their relative motion, and must have its instant screw axis, I_{AS}, located on the Plücker conoid $\mathcal{C}$.

Thus, the choice of the auxiliary surface is not free, since the spatial version of Camus's theorem must be satisfied, but there are infinitely many canditates, which should be evaluated in terms of specific critera, as reported in [20-25].

For example, even in the planar case, whose hyperboloid pitch surfaces can be substituted by the well-known pitch circles, which represent the centrodes of the relative motion between the pair of gears, infinitely many auxiliary curves can be chosen in agreement with Camus' theorem, but only two types of auxiliary curves are chosen in practice. These curves are circles in the case of cycloidal gears or the pole-tangent line for involute gears.

Morever, in order to generate a pair of conjugate profiles, Camus' theorem can be also applied by considering both envelopes of another curve that is attached to the auxiliary curve during its pure-rolling motion on both centrodes, or pitch circles, respectively. This approach is applied in practice to the manufacture of many types of gears, cylindrical and bevel, circular and non-circular, with cycloidal or involute tooth profiles. This approach and pertinent methods can be also extended and applied to bevel and spatial gears, but the auxiliary surface must be chosen in agreement with Camus' theorem.

This paper focuses on the generation of the tooth flanks of involute-gear pairs with skew axes. Thus, the choice of the auxiliary surface must be addressed to extend the cylindrical and bevel gears with involute tooth profiles to the most general case of skew gears.

Furthermore, the auxiliary surface is represented by a pole-tangent plane for involute cylindrical gears and by a pole-tangent great disk for involute bevel gears, both auxiliary surfaces showing an instant screw axis I_{AS} orthogonal to the I_{32}-axis (ISA) and located on their Plücker conoid. These auxiliary surfaces degenerate into a plane and a disk, respectively. Consequently, the same condition to generate involute gears must be satisfied in the spatial case, which can be proven by applying dual algebra and the Principle of Transference to the spherical case [19] to generate the helicoid-rack. The latter cannot be used as auxiliary surface, because its I_{AS} is not located on the Plücker conoid, even if orthogonal to the ISA and, thus, Camus' theorem is not respected.

Therefore, the instant screw axis I_{AS} of the auxiliary surface for generating a pair of conjugate tooth flanks of skew gears, which can be considered the extension to the spatial case of planar and spherical involute gears, must be orthogonal to the ISA and located on the Plücker conoid, according to the spatial version of Camus' theorem. Under these conditions, there is only one axis, which is usually skew with respect to the ISA. This axis and the ISA intersect each other only when the ISA falls in the midpoint between the two torsal generators of the Plücker conoid, which is obtained in practice when $k = -1$.

The orientation of I_{AS} can be obtained by imposing the orthogonality condition with the ISA:

$$\vartheta_{AS} = \vartheta_2 + \frac{\pi}{2} \tag{8}$$

which is substituted into Eq. (3) to yield the transmission ratio k_{AS} in the form

$$k_{AS} = \frac{\cos\left(\alpha_1 - \vartheta_2\right)}{\cos\vartheta_2} \tag{9}$$

In turn, k_{AS} yields the position b_{AS} of I_{AS} along the X-axis, namely,

$$b_{AS} = \frac{4\sin^2\alpha_1\cos^2\vartheta_2 - \sin 2\alpha_1 \sin 2\vartheta_2}{4\sin^2\alpha_1}\, a_1 \tag{10}$$

Equations (1) to (10) have been implemented in Matlab code to provide some examples, as those shown in Fig. 4, where I_{AS} and the ISA intersect each other (Fig.4a) and are mutually orthogonal (Fig.4b), and in Fig. 5, where I_{AS} and the ISA are orthogonal and skew. Both I_{AS} and I_{32} (ISA) are shown in blue and red, respectively.

In particular, Figs. 4 and 5 show both hyperboloid pitch surfaces $\mathcal{P}_2$ (pink) and $\mathcal{P}_3$ (green) of the driving and driven gears, respectively, along with their Plücker conoid (grey) for the same distance $a_1 = 100$ mm between the I_2 and I_3 axes of rotation (black) and different angles α_1 and transmission ratio k. The other data are: $\alpha_1 = 45°$ and $k = -1$ for the example of Fig. 4, and $\alpha_1 = 90°$ and $k = -2$ for that of Fig.5.

Moreover, the top view of Figs. 4b and 5b illustrate that I_{AS} is orthogonal to the ISA, which makes an angle ϑ_2 with the positive Z-axis (I_2-axis).

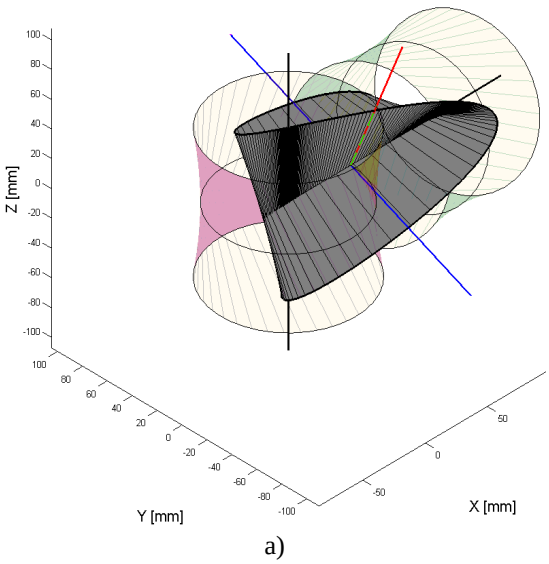

a)

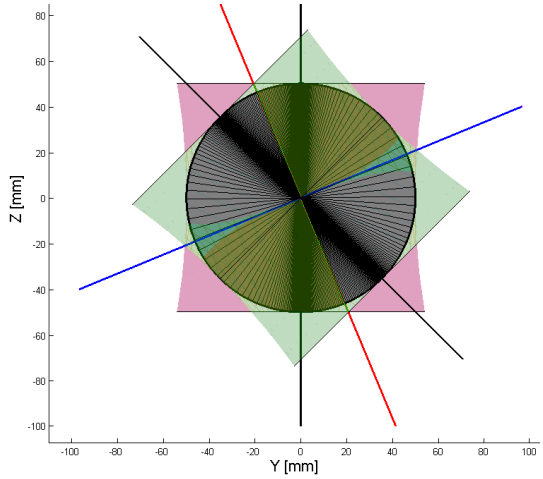

b)

Figure 4. Pitch surfaces, Plücker conoid, the ISA and the I_{AS} of the orthogonal helicoid for a_1 = 100 mm, α_1 = 45°, k = – 1: a) axonometric view; b) top view.

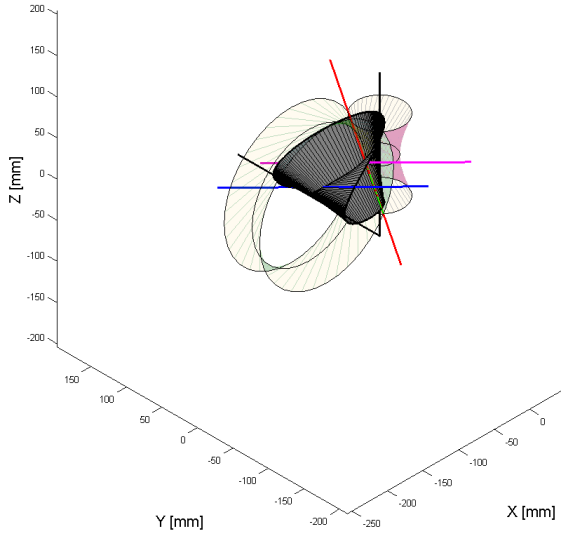

a)

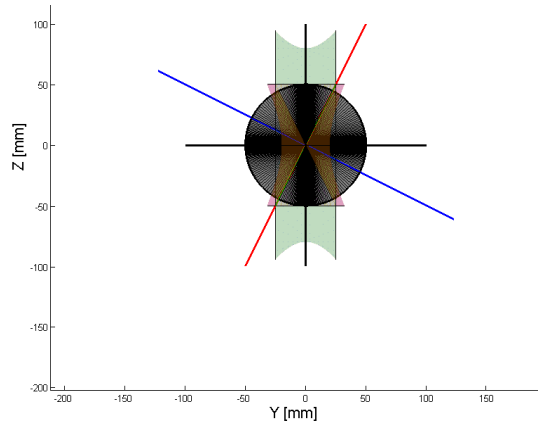

b)

Figure 5. Hyperboloid pitch surfaces, Plücker conoid, the ISA and the I_{AS} of the orthogonal helicoid for a_1 = 100 mm, α_1 = 90°, k = – 2: a) axonometric view; b) top view.

According to Camus' theorem, the auxiliary surface to generate the tooth flanks of involute-gear pairs with skew axes is characterized by the instant screw axis I_{AS}, which is orthogonal the ISA and located on the Plücker conoid.

However, in addition to these geometric properties and in agreement with screw theory, each axis of the Plücker conoid is also associated with a specific pitch $p = v / \omega$, where v and ω are the point and angular velocities, along and around the same axis, respectively. As reported in [19-22], the only two axes with zero pitch are represented by the I_2 and I_3 axes of the gear pair. Thus, the pitch p_{32} of the ISA is given by Eqs. (1) and (2), while the pitch p_{AS} can be obtained by the same equations for $k = k_{AS}$ of Eq. (9).

Consequently, the auxiliary surface to generate the tooth flanks of involute-gear pairs with skew axes takes the form of a right helicoid, since it is generated by the rotation and translation of the ISA around and along the I_{AS}-axis, with angular and point velocities, ω_{AS} and v_{AS}, respectively.

Referring to Fig. 1 and considering a frame $\mathcal{F}_{AS}$ (x_{AS}, y_{AS}, z_{AS}), whose z_{AS} and I_{AS} axes, along with the x_{AS} and X axes, coincide between them, respectively, the homogeneous transformation matrix ${}^{0}\mathbf{T}_{AS}$ from $\mathcal{F}_{AS}$ to $\mathcal{F}_0$ is expressed as

$$ {}^{0}\mathbf{T}_{AS} = \begin{bmatrix} 1 & 0 & 0 & b_{AS} \\ 0 & \cos\vartheta_{AS} & -\sin\vartheta_{AS} & 0 \\ 0 & \sin\vartheta_{AS} & \cos\vartheta_{AS} & 0 \\ 0 & 0 & 0 & 1 \end{bmatrix} \tag{10} $$

where ϑ_{AS} and b_{AS} are given by Eqs. (8) and (10), respectively.

Thus, the central curve of this orthogonal helicoid (AS), which is a helix in general and a straight line in particular, can be obtained by referring the intersection point between the ISA and the X-axis with respect to the $\mathcal{F}_{AS}$ frame, through the position vector $\mathbf{p}_{AS}$, which can be expressed in homogeneous form as

$$ \mathbf{p}_{AS} = \begin{bmatrix} (b_2 - b_{AS})\cos\gamma \\ (b_2 - b_{AS})\sin\gamma \\ \mu \\ 1 \end{bmatrix} \tag{11} $$

where the angle γ and the displacement μ represent the rotation and the translation of $\mathbf{p}_{AS}$, around and along the I_{AS}-axis, respectively. These parameters depend both on time through the constant angular and point velocities ω_{AS} and v_{AS}, respectively.

Therefore, the central helix of the orthogonal helicoid (AS) can be expressed with respect to the fixed $\mathcal{F}_0$ frame by

$$ {}^{0}\mathbf{p}_{AS} = {}^{0}\mathbf{T}_{AS}\,\mathbf{p}_{AS} \tag{12} $$

where ${}^{0}\mathbf{T}_{AS}$ and $\mathbf{p}_{AS}$ are given by Eqs. (10) and (11), respectively. In particular, when $k = k_{AS} = \pm 1$, one has $b_2 = b_{AS}$ and the central helix takes the shape of a straight line.

Likewise, the orthogonal helicoid that represents the ruled auxiliary surface, can be expressed in point coordinates and with respect to the $\mathcal{F}_{AS}$ frame by introducing the parameter $\lambda \in \mathbb{R}$. Moreover, the position vector $\mathbf{p}^*_{AS}$ of a point of the ISA, during its relative motion around and along the I_{AS}-axis, takes the form

$$\mathbf{p}^*_{AS} = \begin{bmatrix} (b_2 - b_{AS})\cos\gamma \\ (b_2 - b_{AS})\sin\gamma \\ \mu \\ 1 \end{bmatrix} + \lambda \begin{bmatrix} \sin\gamma \\ \cos\gamma \\ 0 \\ 1 \end{bmatrix} \qquad (13)$$

In particular, the central helix is obtained for $\lambda = 0$, while the equation of the ISA is given for $\gamma = \mu = 0$ because the ISA is parallel to the y_{AS}-axis at the starting position of the generating motion, as shown in Fig. 2.

Finally, the orthogonal helicoid can be expressed with respect to the fixed frame $\mathcal{F}_0$ by the position vector $\mathbf{p}^*_{AS}$ upon multiplication by the transformation matrix ${}^0\mathbf{T}_{AS}$.

Equations (10) to (13) have been implemented in Matlab code in order to test and visualize the orthogonal helicoid to generate the tooth flanks of involute-gear pairs with skew gears. This ruled surface is shown (yellow) in the examples of Figs. 6 and 7 for different input data. In particular, Fig. 6 shows the case in which I_{AS} intersects the ISA at the midpoint of the common normal between the I_2 and I_3 axes and, consequently, the central helix takes the form of a straight line that coincides with I_{AS}. This condition is satisfied for $k = \pm 1$.

Conversely, the example of Fig. 7 shows a different case for $k = -2$, which yields a central helix (black) with I_{AS} skew and orthogonal to the ISA. Consequently, the orthogonal helicoid is tangent to a cylinder of axis I_{AS} and radius $r = |\, b_2 - b_{AS}\,|$ by assuming the typical shape of a spiral staircase.

Figures 8 and 9 refer to the cylindrical and bevel gears, where the cylindroid degenerates into a plane and a disk, respectively.

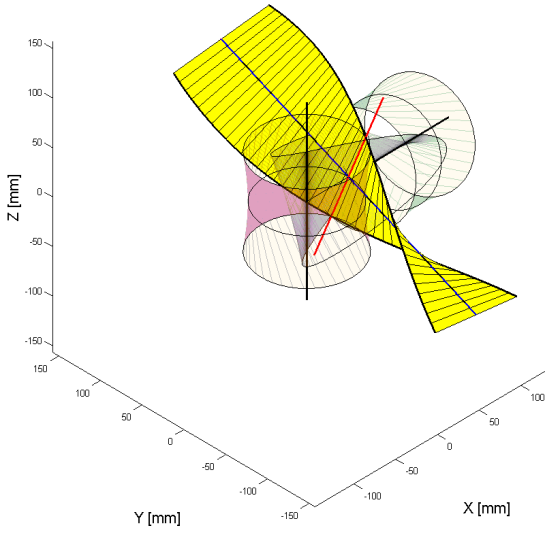

Figure 6. Orthogonal helicoid (AS), along with both hyperboloid pitch surfaces and their Plücker conoid for $a_1 = 100$ mm, $\alpha_1 = 45°$, $k = -1$.

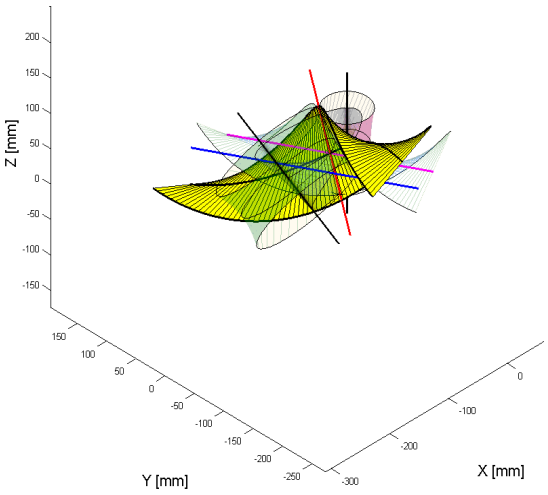

Figure 7. Orthogonal helicoid (AS), along with both hyperboloid pitch surfaces and their Plücker conoid for $a_1 = 100$ mm, $\alpha_1 = -60°$, $k = -2$.

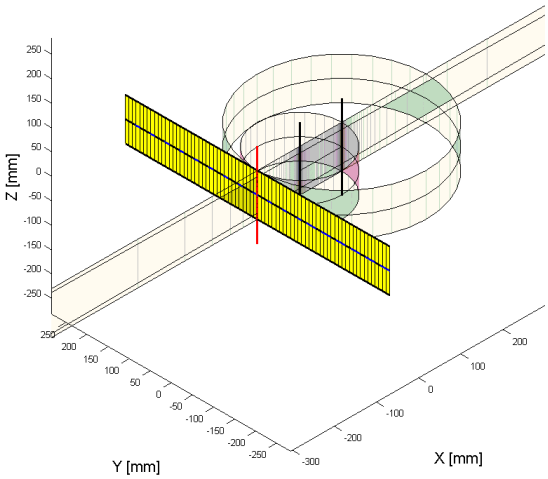

Figure 8. Cylindrical gears: $a_1 = 100$ mm, $\alpha_1 = 0°$, $k = +2$.

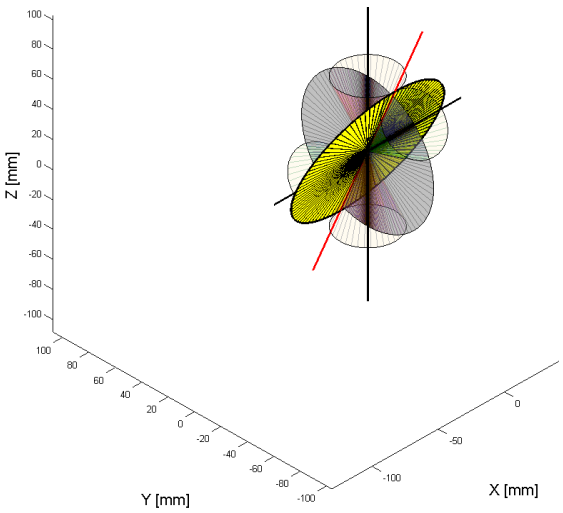

Figure 9. Bevel gears: $a_1 = 100$ mm, $\alpha_1 = 45°$, $k = -1$.

4 SYNTHESIS OF THE INVOLUTE TOOTH FLANKS

The synthesis of the tooth flanks of involute-gear pairs with skew axes is conducted by applying the spatial version of Camus's theorem when the synthesized orthogonal helicoid of Eq. (13) is used as auxiliary surface.

Involute gears were discovered by Leonhard Euler by means of the original sketch of Fig. 10, as reported and extensively described in [26] and [27]. In particular, *A* and *B* are the centers of rotation of the wheels, while *Q* and *P* are the centers of curvature of the conjugate profiles in contact at point *O*, *NOF* and *EOM*, respectively. Euler argued that the common normal at the contact point *O* intersects the joining line across the centers *A* and *B* in the fixed point *T*, in order to respect the condition of a constant velocity ratio.

Consequently, Euler discovered the involute gears and an expression that is nowadays known as the Euler-Savary equation, which finds many more applications in all kinematics than expected by Euler himself. In particular, when the centers of curvature *Q* and *P* become coincident with points *S* and *R*, respectively, the conjugate profiles *EOM* and *NOF* become involute arcs of the pitch circles of the two wheels of centers *A* and *B*, respectively.

Likewise, in the spatial case, during the engagement of both hyperboloid pitch surfaces $\mathcal{P}_1$ and $\mathcal{P}_2$, the orthogonal helicoid (AS) will move accordingly by remaining tangent to them along the ISA, which is fixed in space for constant values of the transmission ratio *k*. Their instant screw axes I_2, I_3 and I_{AS}, along with the ISA (I_{32}), will remain located in the same position on the Plücker conoid.

Moreover, while $\mathcal{P}_1$ and $\mathcal{P}_2$ undergo pure rotation around their I_2 and I_3 axes, the orthogonal helicoid moves through a screw motion with pitch p_{AS}, thus producing rotation and sliding along the ISA.

Thus, according to Camus' theorem, a pair of conjugate tooth flanks can be generated by considering a tracing line of the orthogonal helicoid during its relative motion with respect to $\mathcal{P}_1$ and $\mathcal{P}_2$, respectively.

Referring to the sketch of Fig. 11, different reference frames have been chosen in order to express the position vector of the central helix of the orthogonal helicoid with respect to the driving and driven gears, respectively.

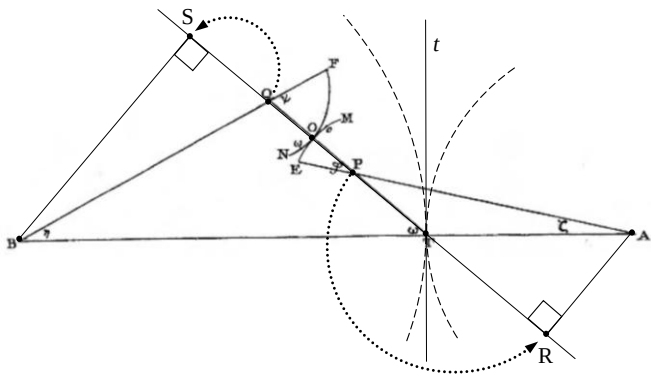

Figure 10. Euler's sketch to find a pair of conjugate profiles (involutes of circles) that yield a constant transmission ratio.

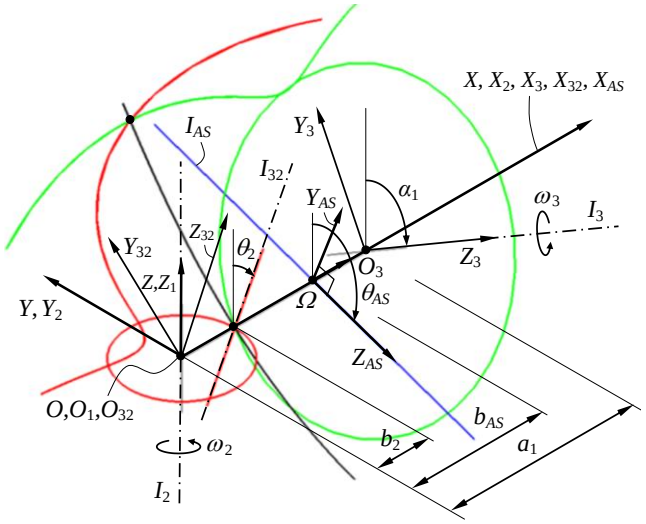

Figure 11. Orthogonal helicoid (AS), along with both hyperboloid pitch surfaces and their Plücker conoid for $a_1 = 100$ mm, $\alpha_1 = 45°$, $k = -1$.

In fact, during their engagement, a point of the central helix will trace two skew profiles, which represent the central curves of the conjugate tooth flanks.

Thus, the position vector of this point can be expressed as

$$\mathbf{p}_{f_s} = {}^{0}\mathbf{T}_{1}\ {}^{1}\mathbf{T}_{32}\ {}^{32}\mathbf{T}_{m}\ \mathbf{p}^{*}_{AS_m} \tag{14}$$

with the transformation matrices ${}^{0}\mathbf{T}_1$, ${}^{1}\mathbf{T}_{32}$ and ${}^{32}\mathbf{T}_m$ given below:

$${}^{0}\mathbf{T}_{1} = \begin{bmatrix} \cos(-\psi) & -\sin(-\psi) & 0 & 0 \\ \sin(-\psi) & \cos(-\psi) & 0 & 0 \\ 0 & 0 & 1 & 0 \\ 0 & 0 & 0 & 1 \end{bmatrix} \tag{15}$$

$${}^{1}\mathbf{T}_{32} = \begin{bmatrix} 1 & 0 & 0 & 0 \\ 0 & \cos\vartheta_2 & -\sin\vartheta_2 & 0 \\ 0 & \sin\vartheta_2 & \cos\vartheta_2 & 0 \\ 0 & 0 & 0 & 1 \end{bmatrix} \tag{16}$$

and

$${}^{32}\mathbf{T}_{m} = \begin{bmatrix} \cos\gamma & 0 & -\sin\gamma & b_{AS} \\ 0 & 1 & 0 & \mu \\ \sin\gamma & 0 & \cos\gamma & 0 \\ 0 & 0 & 0 & 1 \end{bmatrix} \tag{17}$$

Likewise, the position vector of the same point can be expressed as

$$\mathbf{p}_{f_{S_C}} = {}^{0}\mathbf{T}_{3}\ {}^{3}\mathbf{T}_{1C}\ {}^{1C}\mathbf{T}_{32_C}\ {}^{32_C}\mathbf{T}_{m}\ \mathbf{p}^{*}_{AS_m} \tag{18}$$

the transformation matrices ${}^{0}\mathbf{T}_{3}$, ${}^{3}\mathbf{T}_{1C}$, ${}^{1C}\mathbf{T}_{32C}$ and ${}^{32C}\mathbf{T}_{m}$ being, in turn,

$$ {}^{0}\mathbf{T}_{3} = \begin{bmatrix} 1 & 0 & 0 & a_1 \\ 0 & \cos\alpha_1 & -\sin\alpha_1 & 0 \\ 0 & \sin\alpha_1 & \cos\alpha_1 & 0 \\ 0 & 0 & 0 & 1 \end{bmatrix}, \tag{19} $$

$$ {}^{3}\mathbf{T}_{1C} = \begin{bmatrix} \cos(-\varphi) & -\sin(-\varphi) & 0 & 0 \\ \sin(-\varphi) & \cos(-\varphi) & 0 & 0 \\ 0 & 0 & 1 & 0 \\ 0 & 0 & 0 & 1 \end{bmatrix}, \tag{20} $$

$$ {}^{1C}\mathbf{T}_{32_C} = \begin{bmatrix} 1 & 0 & 0 & 0 \\ 0 & \cos(\vartheta_2 - \alpha_1) & -\sin(\vartheta_2 - \alpha_1) & 0 \\ 0 & \sin(\vartheta_2 - \alpha_1) & \cos(\vartheta_2 - \alpha_1) & 0 \\ 0 & 0 & 0 & 1 \end{bmatrix} \tag{21} $$

and

$$ {}^{32_C}\mathbf{T}_{m} = \begin{bmatrix} \cos\gamma & 0 & -\sin\gamma & (b_{AS} - a_1) \\ 0 & 1 & 0 & \mu \\ \sin\gamma & 0 & \cos\gamma & 0 \\ 0 & 0 & 0 & 1 \end{bmatrix} \tag{22} $$

Similar to the derivation of the orthogonal helicoid, both ruled surfaces are obtained through the parameter λ.

5 OSCULATING RULED SURFACES

Two ruled surfaces are osculating when they share the same contact line and tangent plane, but they may intersect each other when they also share the same axis of curvature, which is also known as the Disteli axis, as discovered by Martin Disteli at the turn of the 20th century. This condition is verified when there is a second-order, or three-line contact (G^2-continuity).

These properties are better understood by referring to cylindrical ruled surfaces because they can be analyzed by considering planar curves. In fact, two curves are osculating when they share the same osculating circle and, thus, the same center of curvature, which shows three-point contact with the curve. These two curves osculate, or kiss each other, by giving a more intimate contact than the simple tangency that gives only two-point contact.

Usually, the osculating circle intersects the curve because of the second-order contact, which is even, but they do not intersect each other when the evolute of the curve shows a cusp or the curvature is stationary, because also the first derivatives of the curvature are equal in this case. This means that a third-order contact, which is of odd order, occurs. This concept can be extended to yield the Four-Vertex Theorem, which states that the curvature function of a simple, closed, smooth planar curve, as the ellipse, has at least two local maxima and two local minima.

Referring to [28-32], and according to Camus' theorem, a pair of conjugate profiles can be generated by choosing a tracing point of the pole-tangent, which plays the role of the auxiliary curve to produce involute teeth. These profiles are involutes of the pitch circles and share the same center of curvature, which coincides with the instant center of rotation for the relative motion between the gear pair. This is also the tangent point among the pitch circles and the pole-tangent.

These involute tooth profiles show a G^2-continuity while intersecting each other, and cannot be used in practice because of penetration. This is why the synthesis of involute gears is conducted by means of the extended version of Camus' theorem, which considers the envelope profiles of a second curve that is attached to the auxiliary curve. The simplest choice in practice is a straight line attached to the pole-tangent (auxiliary curve) to generate involute profiles of the base circles instead of the pitch circles.

This approach can be extended to the spatial case by considering the orthogonal helicoid as auxiliary surface and by choosing on it a tracing line analogy with the planar case. However, the same problem of the osculating curves appears in the involute tooth flanks, as osculating ruled surfaces.

This aspect is made apparent in Section 6 through the examples below, obtained with the procedure described here.

6 EXAMPLES

The described procedure was implemented in Matlab to generate the tooth flanks of involute gear pairs with skew axes, the orthogonal helicoid, the Plücker conoid and both hyperboloid pitch surfaces, along with their helicoid-rack. In order to illustrate only the objects of interest, each of them can become transparent because of suitable sliders that appear on the screen when the program runs.

Likewise, the input parameters a_1, α_1 and k can be set and changed in real-time via software through similar sliders and congruent animations of all objects can be run, while showing their relative engagement. In fact, while hyperboloids rotate by touching along the ISA and move both the helicoid-rack and the orthogonal helicoid, the involute tooth flanks engage upon sharing the same tangent plane along a line of contact, which lies on the orthogonal helicoid.

These tooth flanks penetrate each other because of the G^2-continuity and, thus, they are not realizable in practice, but this formulation represents a fundamental step toward the synthesis of involute skew gears with line contact and in agreement with Camus' theorem.

Some examples are shown in Figs. 12 to 17 by setting different values of the input parameters and with the aim to illustrate the line of contact between the tooth flanks. Moreover, as expected, the well-known condition of intersecting flanks or profiles in the case of cylindrical gears is verified by referring to Figs. 15 and 16.

In fact, both involute profiles have the same center of curvature that coincides with the instant center of rotation because these profiles osculate each other by showing a third order of contact without intersecting the osculating circle.

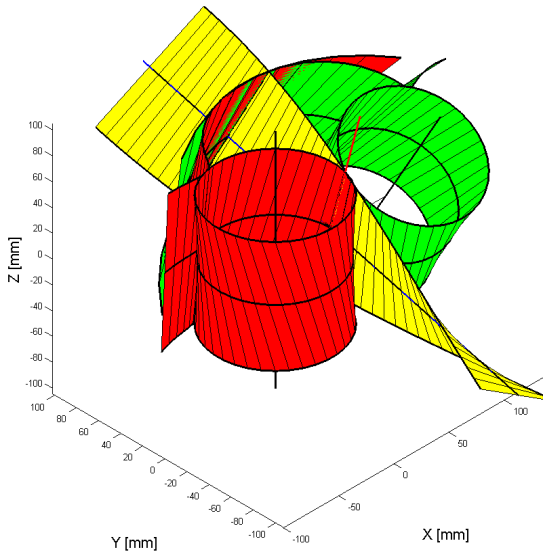

Figure 12. Involute tooth flanks, **o**rthogonal helicoid and both pitch hyperboloids for a_1 = 100 mm, α_1 = 30°, k = – 1.

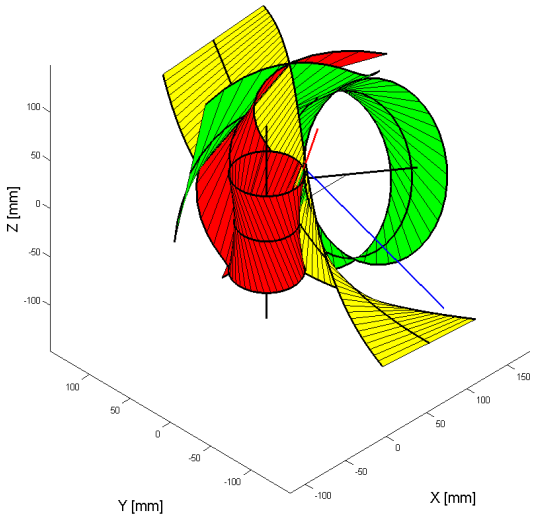

Figure 13. Involute tooth flanks, **o**rthogonal helicoid and both pitch hyperboloids for a_1 = 100 mm, α_1 = 60°, k = – 2.

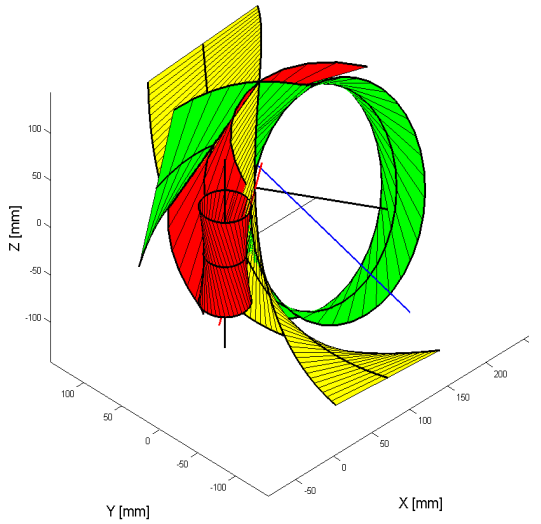

Figure 14. Involute tooth flanks, **o**rthogonal helicoid and both pitch hyperboloids for a_1 = 120 mm, α_1 = 70°, k = – 3.

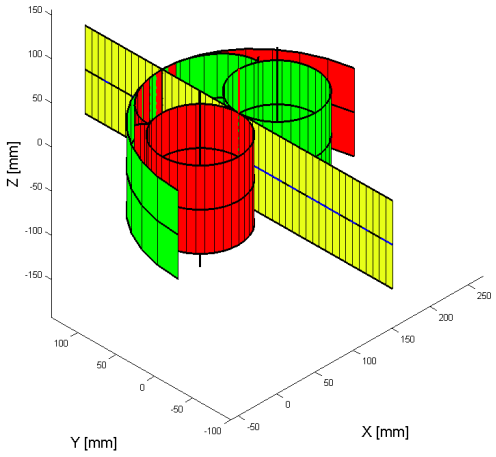

Figure 15. Involute tooth flanks, **o**rthogonal helicoid and both pitch hyperboloids for a_1 = 100 mm, α_1 = 0°, k = – 1.

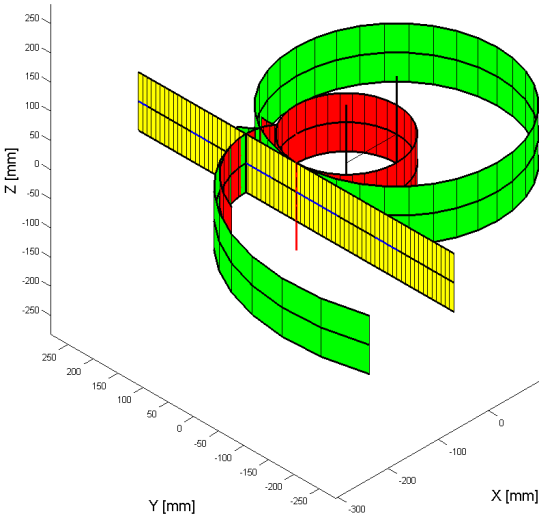

Figure 16. Involute tooth flanks, **o**rthogonal helicoid and both pitch hyperboloids for a_1 = 100 mm, α_1 = 0°, k = + 2.

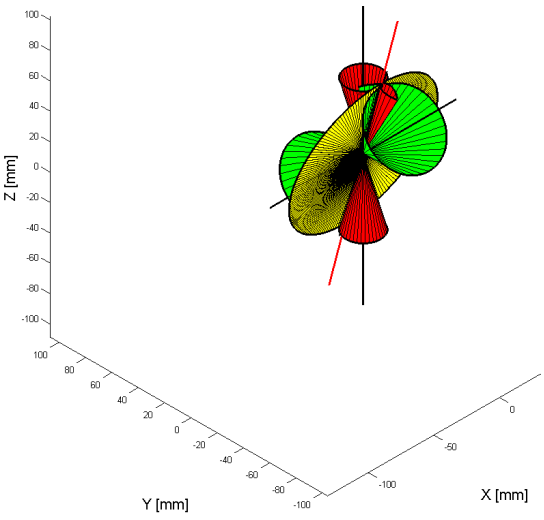

Figure 17. Involute tooth flanks, **o**rthogonal helicoid and both pitch hyperboloids for a_1 = 0, α_1 = 45°, k = – 2.

7 CONCLUSIONS

The role of the orthogonal helicoid in the generation of the tooth flanks of involute gear pairs with skew axes is explained and analyzed through the formulation of a pertinent procedure, implemented in Matlab, and applied to representative examples.

Similar to the planar and spherical cases, the use of a tracing line of the orthogonal helicoid to generate a pair of involute tooth flanks gives conjugate ruled surfaces with line contact, but they are even osculating at particular points (G^2-contact). Thus, these profiles are not realizable in practice.

Nevertheless, this is a fundamental step towards the synthesis of the flanks of involute gears with skew axes.

8 ACKNOWLEDGEMENTS

The third author acknowledges the support received trough his James McGill Professorship. The work reported here was possible under the McGill University-Università di Cassino Collaboration Agreement. The biographical data on Martin Disteli was graciously provided by Prof. Dr. Michael von Renteln, of Karlsruhe University.

REFERENCES

[1] Fueter R., 1923, "Martin Disteli", Vierteljahreszeit-schrift der Naturforschenden Gesellschaft in Zürich, **68**, pp. 593–596.

[2] Generallandesarchiv Karlsruhe Akte N.448/2359.

[3] Mollet H., 1961, "Dr. Martin Disteli, Hochschulprofessor 1862-1923", Oltner Neujahrsblätter, Kommissionsverlag, Olten, pp. 39–42.

[4] Schur F., 1927, "Nachruf auf Martin Disteli, Jahresber, DMV, **36**, pp. 170–173.

[5] Frei G. and Stammbach U., 1994, "Die Mathematiker an den Zürcher Hochschulen, Birkhäuser Verlag, Basel, pp. 23–23.

[6] Disteli M., 1898, "Über Rollkurven und Rollflächen", Zeitschrift fur Mathematik und Physik, **43**, pp. 1–35.

[7] Disteli M., 1901, "Über Rollkurven und Rollflächen", Zeitschrift fur Mathematik und Physik, **46**, pp. 134–181.

[8] Disteli M., 1904, "Über instantane Schraubengeschwindigkeiten und die Verzahnung der Hyberboloidräder", Zeitschrift fur Mathematik und Physik, **51**, pp. 51–88.

[9] Disteli M., 1911, " Über die Verzahnung der Hyperboloidräder mit geradlinigem Eingriff", Zeitschrift fur Mathematik und Physik, **59**, pp. 244–298.

[10] Disteli M., 1914, "Über das Analogon der Savaryschen Formel und Konstruktion in der kinematischen Geometrie des Raumes", Zeitschrift fur Mathematik und Physik, **62**, pp. 261–309.

[11] Tölke J., 1976, "Contributions to the Theory of the Axes of Curvature", Mechanism and Machine Theory, **11** (2), pp.123–130.

[12] Veldkamp J.R., 1976, "On the use of Dual Numbers, Vectors and Matrices in Instantaneous Spatial Kinematics", Mechanism and Machine Theory, **11** (3), pp. 141–156.

[13] McCarthy J.M. and Roth B., 1981, "The Curvature Theory of Line Trajectories in Spatial Kinematics", ASME J. of Mechanical Design, **103** (4), pp. 718–724.

[14] McCarthy J.M., 1987, "On the Scalar and Dual Formulations of the Curvature Theory of Line Trajectories", ASME J. of Mechanisms, Transmissions, and Automation in Design, **109** (1), pp. 101–109.

[15] Phillips J., 2003, General Spatial Involute Gearing, Springer, Berlin.

[16] Stachel H., 2004, "On Spatial Involute Gearing", Proc. of the 6th International Conference on Applied Informatics, Eger, Hungary, pp. 27–39.

[17] Litvin F.L. and Fuentes A., 2004, Gear Geometry and Applied Theory, Cambridge University Press, Cambridge.

[18] Dooner D.B., 2012, Kinematic Geometry of Gearing (Second Edition), John Wiley & Sons, Ltd., Chichester, West Sussex, UK.

[19] Beggs, J.S., 1959, Ein Beitrag zur Analyse r¨aumlicher Mechanismen, Dr.-Ing. Dissertation, Technische Hochschule Hannover, Hanover, Germany.

[20] Figliolini G. and Angeles J., 2006, "The Synthesis of the Pitch Surfaces of Internal and External Skew-Gears and Their Racks", ASME J. of Mechanical Design, **128** (4), pp. 794–802.

[21] Figliolini G., Stachel H. and Angeles J., 2007, "A New Look at the Ball-Disteli Diagram and its Relevance to Spatial Gearing", Mechanism and Machine Theory, **42 (**10), pp. 1362–1375.

[22] Figliolini G., Stachel H. and Angeles J., 2013, "On the Synthesis of Spatial Cycloidal Gears", Meccanica, **48** (5), pp. 1239–1249.

[23] Figliolini G., Stachel H. and Angeles J., 2013, "On Martin Disteli's Spatial Cycloidal Gearing", Mechanism and Machine Theory, **60**, pp. 73–89.

[24] Reuleaux F., 1963, The Kinematics of Machinery, Dover Publications, Inc., New York, pp. 152–154.

[25] Camus Ch.E.L., 1759, Cours de Mathématique: Elements de Mécanique Statique, Second Volume, Durand, Paris, pp. 327–329.

[26] Koetsier T., 2007, "Euler and Kinematics", In: Leonard Euler: Life, Work and Legacy, Bradley R.E. & Sandifer C.E. (Eds.), Elsevier, Amsterdam, pp. 167–194.

[27] Dooner D.B and Griffis M.W., 2007, "On Spatial Euler–Savary Equations for Envelopes", ASME J. of Mechanical Design, **129** (8), pp. 865–875.

[28] Sesini O., 1955, Meccanica Applicata alle Macchine: Cinematica, Ed. Ambrosiana, Milano, pp. 79–80.

[29] Ferrari C. and Romiti A., 1966, Meccanica Applicata alle Macchine, Ed. UTET, Torino, pp. 91–93.

[30] Scotto Lavina G., 1987, Lezioni di Meccanica Applicata alle Macchine, Ed. Siderea, Roma, pp. 56–57.

[31] Wunderlich W., 1970, Ebene Kinematik, Hochschultaschenbuch 447/447a, Bibliographisches Institut, Mannheim, pp. 212–225.

[32] Stachel H., 2000, "Instantaneous spatial kinematics and the invariants of the axodes", Proc. Ball 2000 Symposium, Cambridge 2000, no. 23.

